Correction of Neurological Disease of Mucopolysaccharidosis IIIB in Adult Mice by rAAV9 Trans-Blood–Brain Barrier Gene Delivery

Haiyan Fu[1,2], Julianne DiRosario[1], Smruti Killedar[1,2], Kimberly Zaraspe[1] and Douglas M McCarty[1,2]

[1]The Center for Gene Therapy, The Research Institute at Nationwide Children's Hospital, Columbus, Ohio, USA; [2]Department of Pediatrics, College of Medicine and Public Health, The Ohio State University, Columbus, Ohio, USA

The greatest challenge in developing therapies for mucopolysaccharidosis (MPS) IIIB is to achieve efficient central nervous system (CNS) delivery across the blood–brain barrier (BBB). In this study, we used the novel ability of adeno-associated virus serotype 9 (AAV9) to cross the BBB from the vasculature to achieve long-term global CNS, and widespread somatic restoration of α-*N*-acetylglucosaminidase (NAGLU) activity. A single intravenous (IV) injection of rAAV9-CMV-hNAGLU, without extraneous treatment to disrupt the BBB, restored NAGLU activity to normal or above normal levels in adult MPS IIIB mice, leading to the correction of lysosomal storage pathology in the CNS and periphery, and correction of astrocytosis and neurodegeneration. The IV delivered rAAV9 vector also transduced abundant neurons in the myenteric and submucosal plexus, suggesting peripheral nervous system (PNS) targeting. While CNS entry did not depend on osmotic disruption of the BBB, it was significantly enhanced by pretreatment with an IV infusion of mannitol. Most important, we demonstrate that a single systemic rAAV9-NAGLU gene delivery provides long-term (>18 months) neurological benefits in MPS IIIB mice, resulting in significant improvement in behavioral performance, and extension of survival. These data suggest promising clinical potential using the trans-BBB neurotropic rAAV9 vector for treating MPS IIIB and other neurogenetic diseases.

Received 7 October 2010; accepted 7 February 2011; published online 8 March 2011. doi:10.1038/mt.2011.34

INTRODUCTION

Mucopolysaccharidosis (MPS) IIIB is a devastating lysosomal storage disease (LSD) caused by autosomal recessive defects in the gene coding a lysosomal enzyme, α-*N*-acetylglucosaminidase (NAGLU).[1] The lack of NAGLU activity disrupts the stepwise degradation of a class of biologically important glycosaminoglycan (GAG), leading to the accumulation of heparan sulfate oligosaccharides in lysosomes in cells of most tissues. Cells throughout the central nervous system (CNS) are particularly affected, resulting in complex secondary neuropathology.[2–9] MPS IIIB infants appear normal at birth, but develop progressive neurological manifestations that lead to premature death.[1,10,11] Somatic manifestations of MPS IIIB occur in all patients, and involve virtually all organs, although they are mild relative to other forms of MPS, such as MPS I, II, and VII.

No treatment is currently available for MPS IIIB. For all of the MPS disorders, therapies have historically been limited to supportive care and management of complications. MPS IIIB is not amenable to either hematopoietic stem cell transplantation or recombinant enzyme replacement therapy, that have been used to treat mostly somatic disorders in patients with MPS I, II, and IV.[1,12,13] This is because the neuropathology of MPS IIIB is global and the blood–brain barrier (BBB) precludes effective CNS access.

For the majority of CNS diseases, effective treatments are rare, since the CNS is located in a well protected environment and isolated by a highly defined anatomical/functional barrier. The BBB is completely formed at birth in humans. In general, the BBB protects the CNS by selectively regulating the transport of molecules/agents from the blood circulation into the CNS or *vice versa*. Likewise, it prevents potential therapeutics from entering the CNS. The BBB remains the most critical challenge to developing therapies for CNS diseases, especially global CNS disorders. Because of the abundance of CNS vasculature and the nature of brain anatomy/physiology, it is logical to believe that targeting the entire CNS can be most effectively achieved by systemic delivery through the vasculature.[14]

Gene therapy has great potential for treating LSDs because the secretion of lysosomal enzymes, including NAGLU, leads to bystander effects, thus reducing the demand for gene transfer efficiency.[1] The adeno-associated virus (AAV) vector system has been a favored gene delivery tool, with demonstrated therapeutic effect in a great variety of disease models. To date, no known pathogenesis has been linked to AAV in humans.[15] Recombinant AAV (rAAV) vectors based on AAV serotype 2 (AAV2) have been used in numerous studies for neurological diseases,[16–19] transducing both neuronal and nonneuronal cells in the CNS, with demonstrated therapeutic benefits in treating MPS and other LSDs in animals,[20–29] and in patients with Parkinson's and Batten's disease.[30,31]

Correspondence: *Douglas M McCarty, The Center for Gene Therapy, The Research Institute at Nationwide Children's Hospital, 700 Children's Drive, Columbus, Ohio 43205, USA. E-mail: douglas.mccarty@nationwidechildrens.org*

In the majority of rAAV-CNS gene therapy studies in LSDs, vectors were delivered by direct intracranial injection, which has limited potential for treating global CNS diseases.[28,29,32] To overcome these obstacles, more efficient delivery approaches have been developed with broad or global transduction, and functional benefits for the neurological disease in adult MPS IIIB mice.[20,23,27] Intravenous (IV) rAAV injection into neonatal MPS I, MPS VII, and MPS IIIB mice led to long-term correction of lysosomal storage in both somatic and CNS tissues.[28,33] However, the BBB may still be permeable in neonatal mice while closed at birth in humans. Previously, we demonstrated in adult MPS IIIB mice, that pretreatment with an IV infusion of mannitol, transiently disrupting the BBB, facilitated the CNS entry of IV delivered rAAV2, resulting in diffuse global CNS transduction and neurological correction.[27]

A new solution for CNS gene delivery may be offered by the recently demonstrated trans-BBB neurotropism of AAV9.[34–36] Vectors based on this serotype are able to cross the BBB unaided in neonate and adult animals. While all AAV serotypes have broad tissue tropism, each shows distinct cell-type specificities and receptor pathways.[36,37] Receptors and coreceptors for several AAV serotypes have been identified, and laminin appears to play a role in AAV9 transduction, though the significance of this for crossing the BBB is not clear.[38] An added benefit to using AAV9 vectors is that pre-existing immunity, which has been a concern for clinical translation, is less common than for AAV2 serotype.[39–41]

In this study, we assessed the therapeutic potential of systemic rAAV9 gene delivery in treating MPS IIIB in adult mice. Using a single IV injection of a rAAV9 vector, we were able to achieve global CNS and widespread somatic restoration of NAGLU activity, the correction of lysosomal storage pathology, and the greatest improvement in functional outcome observed to date.

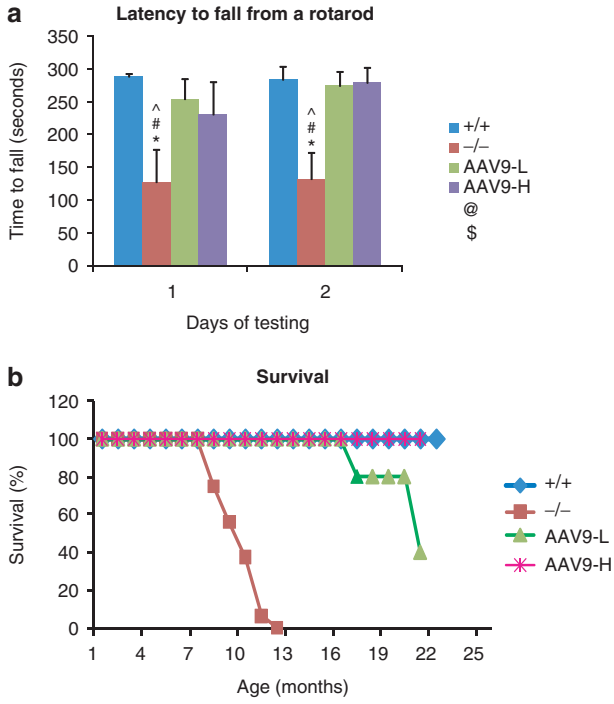

Figure 1 Improved behavior and extended survival in mucopolysaccharidosis (MPS) IIIB mice by systemic recombinant adeno-associated virus 9 (rAAV9) gene transfer. Mice were tested for behavior at 5–5.5 months of age, and were observed for longevity. (**a**) Latency to fall from a rotarod ($n = 11$/group). (**b**) Survival ($n \geq 5$/group, $P < 0.001$). +/+, wt; –/–, MPS IIIB; AAV9-L, AAV9-H, MPS IIIB mice treated with 5×10^{12} or 1.5×10^{13} vg/kg rAAV9-hNAGLU vector, respectively; $^{*}P < 0.05$ (versus +/+); $^{\#}P < 0.05$ (versus AAV9-L); $^{\wedge}P < 0.05$ (versus AAV9-H); $^{\&}P > 0.05$ (versus –/–). NAGLU, α-*N*-acetylglucosaminidase.

RESULTS

To assess the therapeutic efficacy of rAAV9 gene delivery, 4–6-week-old MPS IIIB mice were treated with an IV injection of rAAV9-CMV-hNAGLU (5×10^{12} or 1.5×10^{13} vg/kg, $n = 11$/group). Separately, we treated MPS IIIB mice with 2×10^{13} vg/kg rAAV9-CMV-hNAGLU, with or without mannitol pretreatment ($n = 5$/group), to assess the impact on CNS entry. Controls were sham-treated (phosphate-buffered saline) wild type (wt) and MPS IIIB littermates ($n = 11$). Tissue analyses were carried out at 6 months and 9 months ($n = 2$–4/group) postinjection (pi). Additionally, self-complementary AAV (scAAV) vector carrying a cytomegalovirus-green fluorescent protein (CMV-GFP) transgene (5×10^{12} vg/kg) was injected IV into 6–8-week-old wt mice ($n = 4$/group) to determine the distribution of transgene expression (1 month pi), as a comparison to rAAV9-hNaGlu treatment.

Neurological benefits: correction of cognitive and motor function, and prolonged survival

All mice treated IV with 5×10^{12} or 1.5×10^{13} vg/kg rAAV9-NAGLU were tested for behavior at 5–5.5 months of age to assess the neurological impacts. Both dosage groups exhibited significantly longer latency to fall from an accelerating rotarod (**Figure 1a**), compared with nontreated MPS IIIB mice, indicating the correction of behavioral function. There were no significant differences in behavior performance between these two dose groups.

Ten rAAV9-treated MPS IIIB mice, five from each dose group, were observed for longevity. All 10 survived >16 months (ongoing, with one mouse of the low-dose group dying at age of 16.1 months) while all nontreated MPS IIIB mice died at 8–12 months of age ($P < 0.001$) (**Figure 1b**). These data demonstrate that a single IV rAAV9 vector injection alone is functionally beneficial in treating the CNS disease and increasing longevity in MPS IIIB mice.

Global CNS and widespread somatic restoration of functional NAGLU

Tissues were analyzed at 6 months and/or 9 months pi by immunofluorescence (IF) and NAGLU activity assay to determine the distribution and level of rAAV9-mediated transgene expression. NAGLU-specific IF was detected throughout the brains of treated mice, in neurons, glia, and abundant endothelial cells in capillaries and larger blood vessels, in an apparently dose–dependent fashion (**Figure 2a**). We did not observe significant differences in the distribution or levels of rNAGLU signal between 6 months and 9 months pi. NAGLU-positive glial cells were not costained with anti-glial fibrillary acidic protein (GFAP) Ab, and were likely to be oligodendrocytes, based on their morphology. Importantly, while rNAGLU IF was observed in the brains of all rAAV9-treated mice, mannitol pretreatment did appear to increase the number of transduced cells in the CNS (**Figure 2a**-B,C).

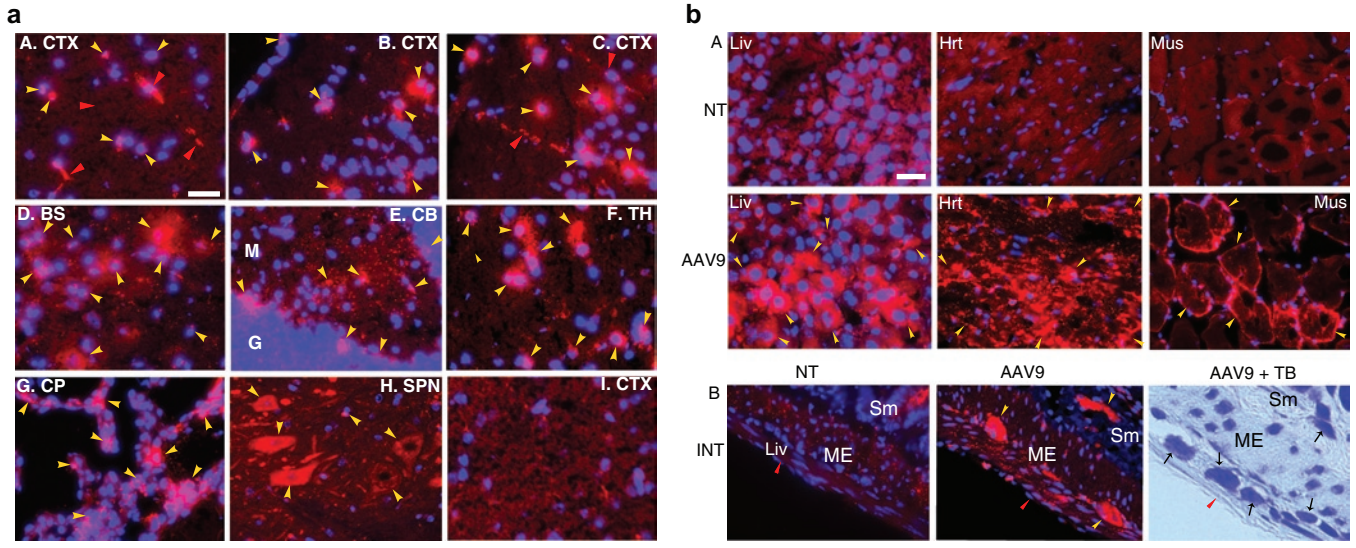

Figure 2 Distribution of recombinant adeno-associated virus 9 (rAAV9)-mediated rNAGLU expression in the central nervous system (CNS) and somatic tissues of mucopolysaccharidosis (MPS) IIIB mice after an intravenous (IV) rAAV9 vector injection. Tissues from rAAV9-CMV-hNAGLU-treated MPS IIIB mice (6 month postinjection) were assayed for hNAGLU by immunofluorescence. Red fluorescence: hNAGLU-positive cells. Blue fluorescence (4′,6-diamidino-2-phenylindole): nuclei. (**a**) CNS; A. mouse treated with 5×10^{12} vg/kg vector; B. mouse treated with 2×10^{13} vg/kg vector; C–H. mouse treated with 2×10^{13} vg/kg vector following mannitol pretreatment; I, nontreated MPS IIIB mouse. BS, brain stem; CB, cerebellum; CP, choroid plexus; CTX, cerebral cortex; SC, spinal cord; TH, thalamus. Yellow arrowheads: hNAGLU-positive brain cells; red arrowheads: hNAGLU-positive endothelial cells. Bar = 100 µm. (**b**) Somatic tissues. Red fluorescence: AAV9, MPS IIIB mouse treated with 2×10^{13} vg/kg vector; NT, nontreated MPS IIIB mouse. A. Hrt, heart; Liv, liver; Mus, skeletal muscle. (quadracep). Yellow arrowheads: hNAGLU-positive cells (hepatocytes, myocytes, cardiomyocytes). B. INT, intestine; ME, muscularis externa; Sm, submucosa; +TB, toluidine blue staining. Yellow arrowheads: rNAGLU-positive neurons of myenteric plexus and submucosal plexus. Red arrowheads: peritoneal surface of intestine. Black arrows: neurons of myenteric plexus and submucosal plexus. Bar = 40 µm. NAGLU, α-*N*-acetylglucosaminidase.

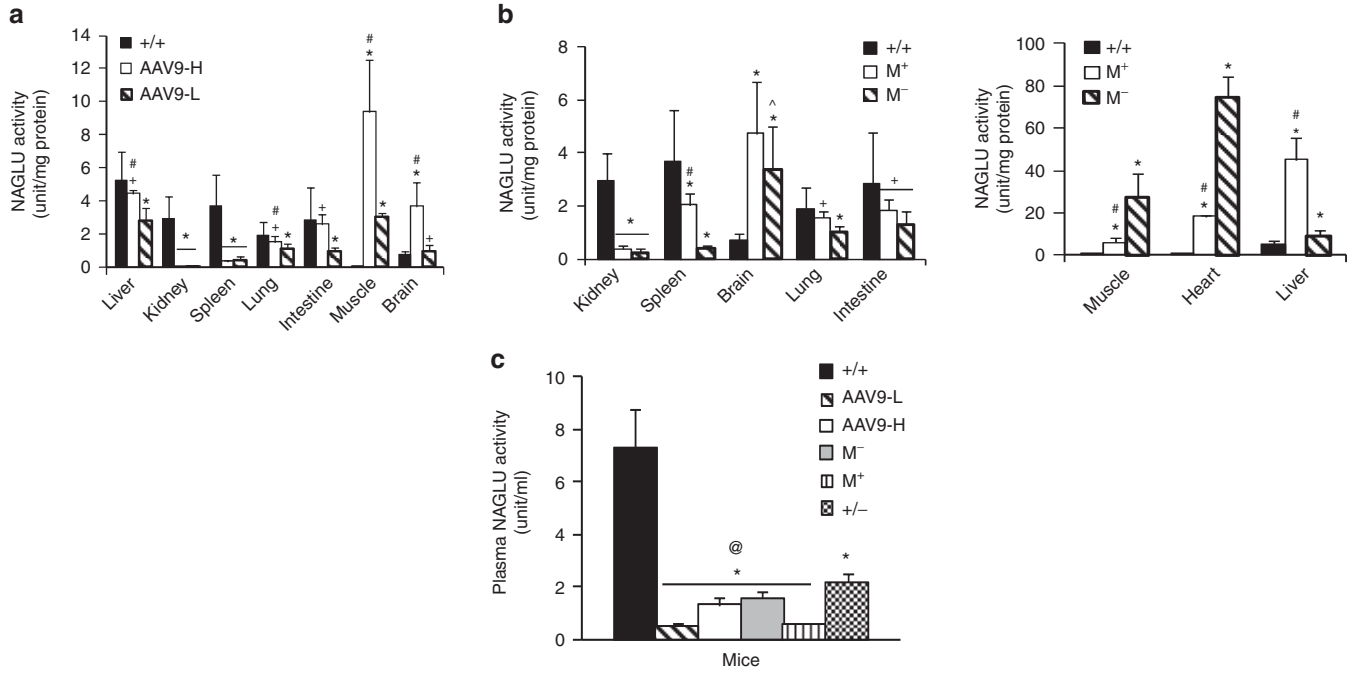

Figure 3 Recombinant adeno-associated virus 9 (rAAV9)-mediated expression of functional rNAGLU in tissues. Tissues from mucopolysaccharidosis (MPS) IIIB mice treated with rAAV9-hNAGLU were assayed for NAGLU activity [6 and 9 months postinfection (pi)] (n = 5–6/group). (**a**) Dose-response. +/+, wt; AAV9-H, AAV9-L, MPS IIIB mice treated with 1.5×10^{13} (AAV9-H) or 5×10^{12} vg/kg (AAV9-L) vector. (**b**) Impact of mannitol pretreatment. M^+/M^-, MPS IIIB mice treated with 2×10^{13} vg/kg vector with (M^+) or without (M^-) mannitol pretreatment. (**c**) Plasma NAGLU activity (n = 3–4). +/–, heterozygotes. No significant difference in tissue NAGLU activity was detected at 6 and 9 months pi. Data shown are means ± SD of combined data on tissues from mice at 6 and 9 months pi. $^*P < 0.01$ versus +/+; $^{\#}P < 0.05$ versus AAV9-L or M^-; $^{+}P > 0.05$ versus +/+. $^{@}P < 0.05$ versus +/–. All P values that were <0.01 and majority of P values that were <0.05, were <0.05 after Bonferroni correction. NAGLU, α-*N*-acetylglucosaminidase.

Differential transduction levels were observed in peripheral organs (**Figure 2b**). The rNAGLU protein was detected in 20–40% of hepatocytes, >95% of cardiomyocytes, and 10–30% of skeletal myocytes (**Figure 2b**-A). The distribution of rAAV9-transduced hepatocytes was uniform throughout the liver. We also observed transduction in abundant neurons in myenteric plexus and submucosal plexus of the intestine (**Figure 2b**-B), suggesting efficient targeting of the peripheral nervous system (PNS). The rNAGLU signals were mostly present in granules (**Figure 2**), whereas scAAV9-mediated GFP signals were uniform in the cytoplasm of transduced cells (**Supplementary Figure S1**), suggesting correct lysosomal trafficking of rNAGLU. Transduction of endothelial cells was also observed in peripheral tissues of rAAV9-GFP vector-treated mice (**Supplementary Figure S1**).

Transgene enzymatic activity was assayed to quantify the expression and the functionality of rAAV9-mediated rNAGLU. We found no significant differences in tissue NAGLU activity at 6 and 9 months pi, suggesting stable transduction. The rAAV-mediated rNaGlu was metabolically functional and the tissue rNAGLU activity was dose-dependent, with approximately normal levels in the brains of mice receiving 5×10^{12} vg/kg vector, and supraphysiologic levels in the brains of mice receiving 1.5×10^{13} vg/kg (**Figure 3a**). In both dose groups, we detected NAGLU activity at normal or subnormal levels in the liver, lung, and intestine (**Figure 3a**), supraphysiologic levels in the skeletal muscles (**Figure 3a**) and heart (40 and 100 units/mg protein, data not shown), and low levels in the spleen, but no detectable NAGLU activity in the kidney (**Figure 3a**). A low level of NAGLU activity was detected in the kidneys of the mice treated with 2×10^{13} vg/kg vector (**Figure 3b**). Mannitol pretreatment led to an increase in NAGLU activity in the brain (though not significant due to high individual variation), liver, spleen, lung, and intestine, but a decrease in the heart and skeletal muscle (**Figure 3b**).

No detectable NAGLU activity (<0.03 unit/mg) was observed in tissues from nontreated MPS IIIB mice.

Plasma rNAGLU: secretion and impact of mannitol

Plasma samples were assayed for NAGLU activity to assess the secretion of the enzyme. Activity was detected in the plasma of all rAAV9-treated MPS IIIB mice at or near heterozygote levels, though lower than homozygous wt levels (**Figure 3c**). Mannitol pretreatment resulted in significant reduction in plasma NAGLU activity. These data indicate that the rNAGLU was secreted, though the source tissue or cell-type is not clear.

Correction of lysosomal storage pathology

Tissues were assayed for GAG content and histopathology to quantify and visualize the impact of IV rAAV9-NAGLU gene delivery on the lysosomal storage pathology in MPS IIIB mice. The single IV rAAV9-NAGLU injection led to a reduction of GAG content to normal levels in the brain, liver, heart, lung, intestine, and skeletal muscle in mice of all four treatment groups (**Figure 4**). Doses of 5×10^{12} vg or 1.5×10^{13} vg/kg resulted in partial GAG reduction in the spleen but had no impact in kidney (**Figure 4a**). Treatment with 2×10^{13} vg/kg led to a decrease of GAG to normal levels in the spleen, and partial GAG reduction in the kidney (**Figure 4b**), consistent with the observed enzyme activity levels.

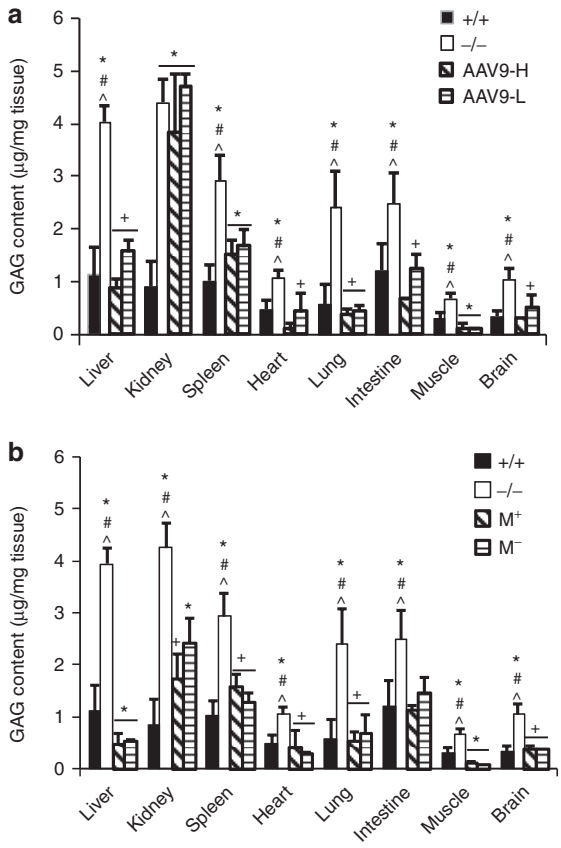

Figure 4 Significant reduction of glycosaminoglycan (GAG) content in the central nervous system and somatic tissues. Tissues from mucopolysaccharidosis (MPS) IIIB mice treated with rAAV9-hNAGLU were assayed to quantify GAG content (6 and 9 months postinfection (pi)). (**a**) Dose-response.(**b**) Impact of mannitol pretreatment. **+/+,** wt; **–/–,** MPS IIIB; AAV9-H, AAV9-L, MPS IIIB mice treated with 1.5×10^{13} vg or 5×10^{12} vg/kg vector; M^+, M^-, MPS IIIB mice treated with recombinant AAV9 vector (2×10^{13} vg/kg) with or without mannitol pretreatment. Data shown are means ± SD (n = 5–6), combining data from tissues collected at 6 and 9 month pi. $^*P < 0.01$ versus +/+; $^\#P < 0.05$ versus AAV9-H or M^+; $^\wedge P < 0.05$ versus AAV9-L or M^-; $^+P > 0.05$ versus +/+. All P values that were <0.01 and majority of P values that were <0.05, were <0.05 after Bonferroni correction. NAGLU, α-*N*-acetylglucosaminidase; rAAV9, recombinant adeno-associated virus 9.

Histopathology showed no lysosomal storage lesions in cells in the vast majority of CNS areas, including cerebral cortex, thalamus, brain stem, hippocampus, and spinal cord in all four treatment groups (**Figure 5a**). There were decreases in the size, number of vacuoles, and number of cells with lysosomal storage lesions, in the few brain areas that showed a lower extent of correction, such as purkinje cells (**Figure 5a**) and cells in the striatum and hypothalamus (data not shown). Importantly, the majority of brain and spinal cord parenchymal cells exhibited a well defined normalized morphology (**Figure 5a**). Immunofluorescence detection for the lysosomal marker, LAMP-1, showed that IV infusion of rAAV9-NAGLU vector at all doses also resulted in marked reduction of LAMP-1 signal, especially in neurons, throughout the brain (**Figure 5b**). This further supports the conclusion that

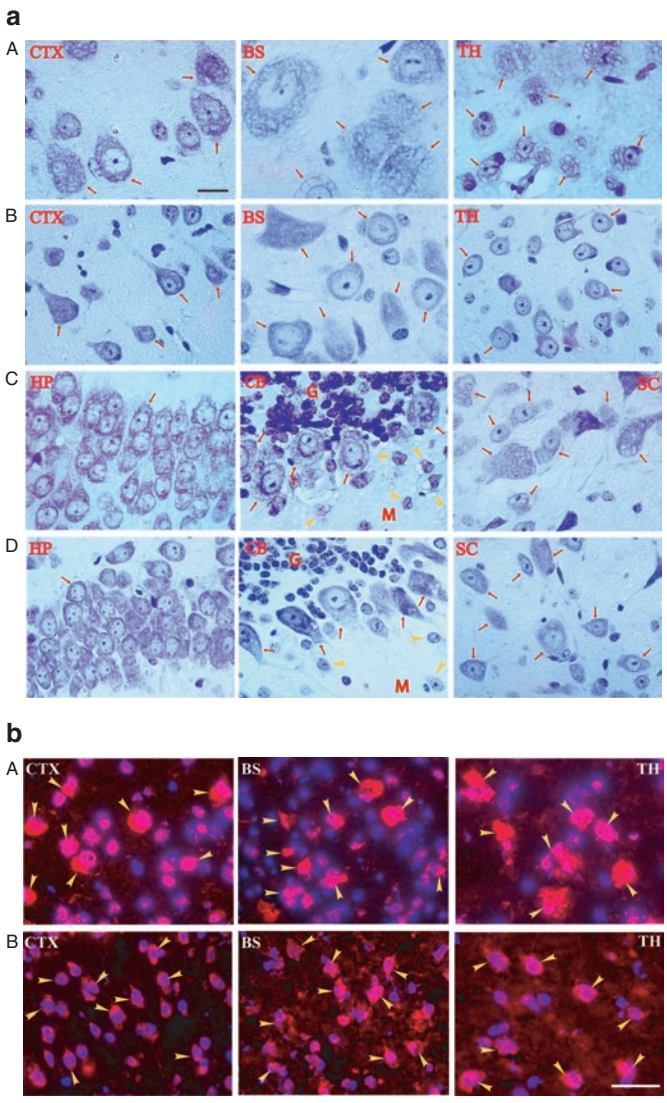

Figure 5 Correction of lysosomal storage pathology in the central nervous system of mucopolysaccharidosis (MPS) IIIB mice after intravenous (IV) recombinant adeno-associated virus 9 (rAAV9) gene delivery. (**a**) Paraffin sections from mice treated with 5 × 10^{12} vg/kg rAAV9-hNAGLU vector [6 months postinfection (pi)] were stained with toluidine blue. The lysosomal storage lesions are shown as vacuoles. A, C. Nontreated MPS IIIB mice; B, D. rAAV9-treated MPS IIIB mice. BS, brain stem; CB, cerebellum; CTX, cerebral cortex (pyramidal layer); G, granular layer of CB; HP, hippocampus; M, molecular layer of CB; SC, spinal cord (ventral horn motor neurons); TH, thalamus; Red arrows and yellow arrowheads, neurons. (**b**) Cryostate brain sections (6 months pi) were assayed for lysosomal-associated membrane protein 1 (LAMP-1) (red fluorescence) by immunofluorescence. A. Nontreated MPS IIIB mouse. B, rAAV-treated MPS IIIB mouse; BS, brain stem; CTX, cerebral cortex (pyramidal layer); TH, thalamus. Yellow arrowheads: LAMP-1-positive cells. Blue fluorescence (4′,6-diamidino-2-phenylindole), nuclei. Bar = 20 µm. NAGLU, α-*N*-acetylglucosaminidase.

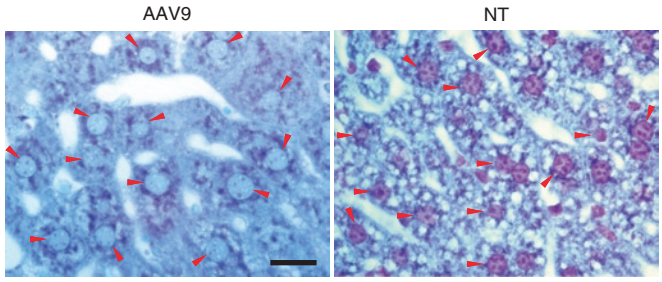

Figure 6 Correction of lysosomal storage pathology in the liver of mucopolysaccharidosis (MPS) IIIB mice after intravenous (IV) recombinant adeno-associated virus 9 (rAAV9) gene delivery. Cryostate liver sections from mice treated with 5 × 10^{12} vg/kg rAAV9-hNAGLU vector (6 months postinfection) were stained with toluidine blue. Lysosomal storage lesions are shown as vacuoles. AAV9, rAAV9-treated MPS IIIB mouse; NT, nontreated MPS IIIB mouse; Red arrowheads, nuclei of hepatocytes. Bar = 20 µm. NAGLU, α-*N*-acetylglucosaminidase.

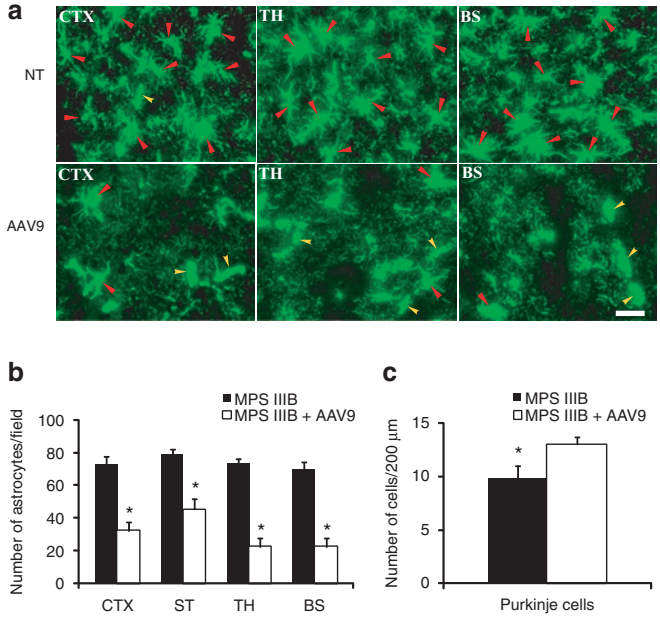

Figure 7 Recombinant adeno-associated virus 9 (rAAV9)-mediated correction of astrocytosis and neurodegeneration in mucopolysaccharidosis (MPS) IIIB mice. Brain sections of MPS IIIB mice treated with rAAV9-CMV-hNAGLU vector (6 months postinfection) were assayed for glial fibrillary acidic protein (GFAP) by (**a**,**b**) immunofluorescence (IF) and (**c**) stained with toluidine blue for histopathology. (**a**) IF images of astrocytes (green fluorescent-$GFAP^+$). (**b**) Number of astrocytes: Data are means ± SD of $GFAP^+$ cells per 330 × 433 µm on 6–8 IF-GFAP-staining sections/mouse, from three mice/group. (**c**) Number of purkinje cells: Data are means ± SD of purkinje cells/200 µm (in length) in ansiform lobules in cerebellum on six toluidine blue stained sections/mouse, from three mice/group. AAV9, MPS IIIB mouse treated with rAAV9; BS, Brain stem; CTX, cerebral cortex; NT, nontreated MPS IIIB mouse; ST, striatum; TH, thalamus. *P < 0.01 versus nontreated. NAGLU, α-*N*-acetylglucosaminidase.

the amount of vector crossing the BBB was sufficient for efficient correction of CNS lysosomal storage pathology.

In somatic tissues, we observed complete clearance of lysosomal storage lesions in the livers of all rAAV9-hNaGlu treated mice and attenuation of nuclear shrinkage, a marker of cell stress and damage (**Figure 6**).

Correction of secondary neuropathology: effects on astrocytosis and neurodegeneration

In order to determine whether IV rAAV9-hNaGlu vector delivery had an impact on astrocytosis, a major secondary neuropathology of MPS IIIB,[6,7] brain sections were assayed by immunofluorescence for GFAP expressing cells. We observed significant decreases

Table 1 Estimated vector genome in the liver and brain of recombinant adeno-associated virus 9 (rAAV9)-treated mice

		Vector genome (copy/cell)		
Mice	*n*	Liver	Brain	Heart
rAAV9-L	2	8.20 ± 4.73	0.07 ± 0.07	0.07[a]
rAAV9-H	3	10.86 ± 2.94	0.09 ± 0.47	0.13 ± 0.07
rAAV9-M$^-$	2	21.97 ± 6.43	0.06 ± 0.001	0.22[a]
rAAV9-M$^+$	3	32.09 ± 3.93	0.15 ± 0.02	0.14[a]
Nontreated	1	0.000	0.000	0.00

Abbreviations: rAAV9-L, intravenous (IV) infusion of 5 × 10^{12} vg/kg; rAAV9-H, IV infusion of 1.5 × 10^{13} vg/kg; rAAV9-M$^-$, IV infusion of 2 × 10^{13} vg/kg without mannitol pretreatment; rAAV9-M$^+$, IV infusion of 2 × 10^{13} vg/kg following mannitol pretreatment.
Mouse tissue samples (6 months postinfection) were assayed in duplicates for vector genome copy numbers by qPCR. Data is expressed as vector copy/cell (means ± SD).
[a]Data from one sample in duplicates.

in astrocyte numbers in gray matter throughout the brain of treated mice compared to untreated at 6 months and 9 months postinjection (**Figure 7a,b**). Histopathology also revealed significant increases in the numbers of neurons, such as Purkinje cells (**Figure 7c**), in the brains of treated MPS IIIB mice. These data strongly indicate the amelioration of astrocytosis and neurodegeneration, which are hallmarks of secondary neuropathologies in MPS IIIB, in response to the rAAV9 treatment.

Differential tissue distribution of rAAV vector genome

Quantitative real-time PCR was performed to compare the amount of rAAV9-CMV-hNaglu vector entering the CNS versus somatic tissues. **Table 1** shows the distribution of the vector genome in different tissues/organs of MPS IIIB mice treated with IV vector injection at varying doses. The highest concentrations of vector genome were detected in liver (8.20 ± 4.73–32.09 ± 3.93 copies/cell), followed by heart (0.07–0.22 copies/cell), and brain (0.06 ± 0.001–0.15 ± 0.02 copies/cell), and very low copy numbers were detected in other tissues/organs (**Table 1**). This differential vector distribution in rAAV9-treated MPS IIIB mice largely correlated with the distribution of rNAGLU IF and enzymatic activity (**Figures 2** and **3**). Notably, mannitol pretreatment increased the vector copy numbers in the brain, correlating with brain NAGLU activity levels. Furthermore, these data reflect persistence of vector genome distribution in treated mice at 6 months pi, supporting a stable long-term transduction. We were unable to detect vector genome copies at levels correlating with rNAGLU activity and distribution in skeletal muscles, possibly due to difficulties in quantitative isolation of DNA from muscle tissue. (**Figures 2** and **3**).

DISCUSSION

Gene delivery vectors derived from the recently characterized AAV9 have unique properties relating to the distribution of transgene expression in animal models, including the ability to cross the BBB from the vasculature.[34,35] In this study, we have demonstrated the first significant therapeutic benefit for treating neurological disorders in adult animals from systemic gene delivery to the CNS without additional treatment to disrupt the BBB. A single IV injection of hNAGLU-expressing rAAV9 vector was sufficient to significantly improve behavioral functions, and greatly prolong survival in MPS IIIB mice. We had previously determined that increased longevity in the MPS IIIB mouse model was highly dependent on the efficiency of gene transfer to the CNS, irrespective of transduction in peripheral tissues and organs.[20,23,27] In this study, using rAAV9, the increased longevity exceeds the outcome of previous studies using rAAV2 vector delivered through either intracisternal injection, or systemic injection following mannitol pretreatment. The rNAGLU enzyme was clearly secreted and functional, leading to a significant bystander effect, and efficient degradation of heparan sulfate GAG in CNS tissues. Importantly, the clinically meaningful therapeutic benefits of the IV delivered rAAV9 vector in MPS IIIB mice were achieved at a lower dose than the mannitol-facilitated, systemically delivered rAAV2 vector.[27] This suggests that using rAAV9 will ease one of the major challenges in mouse-human translation of systemic gene therapy procedures; the scalability of vector production. The enhancement rAAV9-CNS transduction in response to mannitol pretreatment suggests further potential for reducing the vector dose, and the attendant risk and burden to patients.

The IV vector injection resulted in a ubiquitously diffuse, global rAAV9-NaGlu transduction throughout the CNS, reflecting the expected distribution pattern for vascular delivery. This contrasts sharply with the focal gradient distribution typically achieved through direct brain parenchymal injection, or the periventricular transduction pattern from intracisternal and intraventricular injection. While similar to the pattern of transgene expression from IV delivered rAAV2 after mannitol pretreatment, the extent of rAAV9 transduction was significantly higher in all areas of the brain. This correlates with the increased effects on longevity and cognitive function compared to that previously achieved using rAAV2-mannitol treatment, and the normal or above normal levels of NAGLU activity in the CNS. These findings strongly support the potential of the trans-BBB neurotropic rAAV9 as a vector for CNS gene therapy and reinforce the view that efficient CNS delivery is the most critical issue for developing therapies to treat MPS IIIB and many other neurological diseases.

The rAAV9-transduced CNS cells include neurons, glia, and endothelia. Neuronal cell transduction appears to be nonpreferential, including most types of neurons throughout the brain. In contrast, the transduction of glial cells appears to be cell-type specific, targeting predominantly oligodendrocyte-like cells, though it is unclear whether this is a receptor- or promoter-specific phenomenon. In a previous report describing predominant transduction of astrocytes after systemic injection of rAAV9 vector in adult mice, a hybrid chicken β-actin/CMV-enhancer promoter was used, rather than the CMV enhancer-promoter used in this study.[34]

In normal cells, 5–20% of newly synthesized lysosomal protein is secreted,[42] and available to be taken up by neighboring cells, leading to the bystander effect.[1] While we cannot directly determine whether the rNAGLU detected in each tissue is secreted or not, the widespread clearance/reduction of lysosomal storage pathology, and normalized tissue GAG content, strongly support an efficient bystander effect from the rAAV9-mediated rNAGLU. The abundant transduction of endothelial cells in the brain may be an important contributor to the effectiveness of rAAV9 gene delivery for MPS IIIB, and potentially most other LSDs, because

of the close association between CNS cells and brain microvascular endothelial cells, which together constitute the neurovascular unit. While the observed high levels of rNAGLU expression stem from the transduction of a relatively small number of CNS cells, it is sufficient to correct the neuropathology and lead to functional correction of the neurological disorders.

The rAAV9 treatment also led to a regular morphology in CNS cells, and the correction of major secondary neuropathology, astrocytosis, and neurodegeneration. It is worth noting that we had not achieved this level of correction of CNS pathology in our previous studies using rAAV2-hNAGLU vector with mannitol,[20,23,27] further supporting the effectiveness of the trans-BBB neurotropic properties of rAAV9 for the treatment of global neuropathies. The dose-dependent increase in rAAV9-CNS transduction suggests that greater levels may yet be achieved at higher doses, with the potential to treat neurological diseases that involve nonsecreted proteins, particularly if the more efficient self-complementary AAV vectors can be used.

Although neuropathology is the primary cause of mortality in MPS IIIB patients, somatic correction may provide additional therapeutic benefits, since lysosomal storage pathology inevitably manifests in virtually all organs. The IV delivered rAAV9 exhibited broad tropism in peripheral tissues in a distinct pattern, as previously reported, reflecting extensive extravasation and cell-type specific transduction. This led to complete, long-term correction of lysosomal storage in multiple somatic tissues even at a relatively low-dose. Again, relatively low levels of transduction in some tissues were associated with clearance of lysosomal storage of GAGs in the organs, consistent with a significant contribution from the bystander effect of secreted rNAGLU enzyme. It is not clear whether the bystander correction in peripheral tissues is mediated by enzyme secreted from neighboring cells within the same tissue, or circulating rNAGLU secreted by more extensively transduced tissues, in a manner analogous to enzyme replacement therapy. However, the observation of partial GAG reduction in the kidney only at the highest vector dose, correlating with detectable transduction in the kidney only at that dose, suggests that the bystander effect may be primarily local in this tissue. The primary source of circulating NAGLU may be liver, muscle, or endothelium. However, the decrease in plasma levels in response to mannitol pretreatment correlated with decreased transduction in muscle rather than liver, suggesting that liver may not be the primary source.

While the mechanisms are unclear, the low rAAV9 transduction efficiency in kidney and spleen may be attributed to the lack of the rAAV9-specific receptor in cells and/or the cell-specific function of the promoter. These should be considered when developing AAV9 gene therapy targeting kidney or spleen.

Another important observation is the efficient transduction of neurons in myenteric plexus and submucosal plexus of the intestine, potentially enabling correction of not only the CNS but also the PNS at all levels *via* systemic delivery.[43] This suggests that neurotropism is a general property of the AAV9 serotype, and not dependent on the specific structure of the brain neurovascular unit. Broad neurotropism is a valuable property in gene therapy for the treatment of MPS IIIB, considering that we have recently observed lysosomal storage pathology not only in the CNS but also in the PNS (H. Fu, unpublished data). Optimal therapeutic benefits will likely depend on both the CNS and PNS transgene delivery. This view is supported by a comparison of our previous studies using either delivery of vector by intracisternal injection, or by systemic vector injection following mannitol pretreatment.[20,23,27] Both treatments yielded improvements in longevity and cognitive function, however, improved motor function in the rotarod assay was observed only when systemic vector delivery was involved. This suggests that deficiencies in motor function were only effectively corrected with gene delivery to both the CNS and the periphery.

In summary, the novel trans-BBB neurotropic properties of the rAAV9 vector have yielded the best outcome so far observed in our MPS IIIB gene therapy studies. Our results reinforce the view that efficient CNS gene transfer is the key to treating MPS IIIB, and potentially many other LSDs, though additional therapeutic benefits can be achieved from somatic targeting. The use of rAAV9 vector will address two additional challenges in moving rAAV gene therapy to human applications; scalability of vector production and widespread pre-existing AAV2 immunity. We anticipate that this noninvasive procedure will pose a minimal burden to MPS IIIB patients and will be well suited for clinical application. Mannitol pretreatment can enhance rAAV9-CNS entry, offering further potential for reducing the vector dose, and the attendant risk and burden to patients.

MATERIALS AND METHODS

Recombinant AAV (rAAV) viral vectors. A previously described conventional single-strand rAAV vector plasmid[20,22,23,27] was used to produce rAAV9-CMV-hNAGLU viral vector. A scAAV vector plasmid[21] was used to produce the scAAV9-CMV-GFP vector. The vector genomes contained minimal elements required for transgene expression, including AAV2 terminal repeats, a human CMV immediate-early promoter, simian virus 40 splice donor/acceptor signal, a human NAGLU coding sequence or a *GFP* gene, and simian virus 40 polyadenylation signal. The rAAV9 viral vectors were produced in 293 cells using three-plasmid cotransfection, and purified following published procedures.[44]

Animals. An MPS IIIB knockout mouse colony[45] was maintained on an inbred background (C57BL/6) of backcrosses of heterozygotes in the Vivarium at NCH-RI. All care and procedures were in accordance with the Guide for the Care and Use of Laboratory Animals [DHHS Publication No. (NIH) 85–23]. The genotypes of progeny mice were identified by PCR.

Vector delivery. For injection accuracy, the mice were anesthetized by an intraperitoneal injection of Avertin (0.3–0.4 µg/g body weight) prior to rAAV9 vector (in 150–200 µl phosphate-buffered saline) injection *via* tail vein, either unaccompanied, or at 8 minutes after an IV infusion of mannitol (25%, NDC63323-024-25; Abraxis Pharmaceutical Product, East Schaumburg, IL).[27]

Behavioral tests. The rAAV9-CMV-hNaGlu-treated MPS IIIB mice and controls were tested for behavioral performance at ~5.0–5.5 months of age as follows:

Rotarod: Mice were tested on an accelerating rotarod (Med Associates, St Albans, VT) to assess motor co-ordination.[46] Rotation speed was set at an initial value of three revolutions per minute (rpm), with a progressive increase to a maximum of 30 rpm across 5 minutes (the maximum trial length). For the first test session, animals were given three trials, with 45 seconds between each trial. Two additional trials were given 48 hours later. Measures were taken for latency to fall from the top of the rotating barrel.

Longevity assessment. Following the rAAV9-hNaGlu vector injection(s), mice were continuously observed for the development of end point symptoms, or until death occurred. The end point was when the symptoms of late stage clinical manifestation (urine retention, rectal prolapse, protruding penis) in MPS IIIB mice became irreversible, or when wt control mice were 24 months or older.

Tissue analyses. In therapeutic studies, tissue analyses were carried out at 6 months and 9 months pi. Mice were anesthetized with 2.5% Avertin before tissue collection. Brain, spinal cord, and multiple somatic tissues were collected on dry ice or embedded in optical coherence tomography compound and stored at −70 °C, before being processed for analyzes. Tissues were also processed for paraffin sectioning.

Tissue samples from scAAV9-GFP vector-treated mice were collected for analysis 4–5 weeks pi. The mice were anesthetized with 2.5% Avertin and then perfused transcardially with cold phosphate-buffered saline (0.1 mol/l, pH 7.4), followed by 4% paraformaldehyde in phosphate buffer (0.1 mol/l, pH 7.4). The entire brain and spinal cord, as well as multiple somatic tissues (including liver, kidney, spleen, heart, lung, intestine, and skeletal muscles), were collected and fixed in 4% paraformaldehyde overnight at 4 °C before being further processed for vibratome sectioning.

NAGLU activity assay: Tissue samples were assayed for NaGlu enzyme activity following a published procedure with modification.[45,47] The assay measures 4-methylumbelliferone, a fluorescent product formed by hydrolysis of the substrate 4-methylumbelliferyl-N-acetyl-α-D-glucosaminide. The NaGlu activity is expressed as unit/mg protein. One unit is equal to 1 nmol 4-methylumbelliferone released/hour at 37 °C.

GAG content measurement: GAG was extracted from tissues following published procedures[48] with modification.[20] Dimethylmethylene blue assay was used to measure GAG content.[49] The GAG samples (from 0.5 to 1.0 mg tissue) were mixed with H_2O to 40 µl before adding 35 nmol/l dimethylmethylene blue (cat. no. 03610-1; Polysciences, Warrington, PA) in 0.2 mmol/l sodium formate buffer (pH 3.5). The product was measured using a spectrophotometer (OD_{535}). The GAG content was expressed as µg/mg tissue. Urine GAG content was also measured. Heparan sulfate (H9637; Sigma, St Louis, MO) was used as standard.

Histopathology: Histopathology was performed following standard methods. Paraffin sections (4 µm) were fixed with 4% paraformaldehyde in phosphate buffer (0.1 mol/l, pH 7.2) at 4 °C for 15 minutes and stained with 1% toluidine blue at 37 °C for 30 minutes to visualize lysosomal GAG. The sections were mounted, and imaged under a light microscope.

Immunofluorescence: IF was performed to identify cells expressing hNaGlu, GFP, or GFAP for astrocytes, using antibodies against hNaGlu (a kind gift from Dr EF Neufeld, UCLA), GFP (Invitrogen, Carlsbad, CA) or GFAP (Chemicon, Temecula, CA), and corresponding secondary antibody conjugated with AlexaFluor^{568} or AlexaFluor^{488} (Molecular Probes, Carlsbad, CA). The IF staining was performed on thin cryostat sections (8 µm) of tissue samples following procedures recommended by the manufacturers. The sections were visualized under a fluorescence microscope.

Quantitative real-time PCR: Total DNA was isolated from tissue samples of treated and nontreated MPS IIIB mice using Qiagen DNeasy columns. Brain DNA was isolated from midbrain tissue. The DNA samples were analyzed by quatitative real-time PCR, using Absolute Blue QPCR Mix (Thermo Scientific, Waltham, MA) and Applied Biosystems 7000 Real-Time PCR System, following the procedures recommended by the manufacturer. Taqman primers specific for the CMV promoter were used to detect rAAV vector genomes: f: GGCAGTACATCAAGTGTATC; r: ACCAATGGTAATAGCGATGAC; probe: [6~FAM]AATGACGGTAAATGGCCCGC[TAMRA~6~FAM]. Genomic DNA was quantified in parallel samples using β-actin specific primers: f: GTCATCACTATTGGCAACGA; r: CTCAGGAGTTTTGTCACCTT; probe: [6~FAM]TTCCGATGCCCTGAGGCTCT[Tamra~Q] Genomic DNA from nontreated MPS IIIB mouse tissues was used as controls for background and absence of contamination.

Statistical analyses. Means, SD and unpaired Student's *t*-test were used to analyze quantitative data. Behavioral measures were taken by an observer blind to experimental treatment. *P* values generated from *t*-tests were further analyzed individually using Bonferroni correction. Behavioral testing data were also analyzed using repeated measures ANOVA (SAS 9.1.3; SAS Institute, Cary, NC) to determine the significance of the variances among treatment and control groups and testing days. Longevity data were analyzed using Kaplan–Meier method. The significance level was set at $P < 0.05$.

SUPPLEMENTARY MATERIAL

Figure S1. Distribution of rAAV9-mediated GFP expression in the CNS and periphery of MPS IIIB mice after an IVrAAV9 injection.

ACKNOWLEDGMENTS

We thank Ben's Dream–The Sanfilippo Research Foundation for their generous support over the years. We also thank William Gardner and Wei Wang at the Biostatistics Core in the Research Institute at Nationwide Children's Hospital for providing statistical analyses.

REFERENCES

1. Neufeld, EF and Muenzer, J (2001). The mucopolysaccharidoses. In: Scriver, CR, Beaudet, AL, Sly, WS and Valle, D (eds). *The Metabolic & Molecular Basis Of Inherited Disease*, 8th edn. McGraw-Hill: New York; St Louis; San Francisco. pp 3421–3452.
2. Ryazantsev, S, Yu, WH, Zhao, HZ, Neufeld, EF and Ohmi, K (2007). Lysosomal accumulation of SCMAS (subunit c of mitochondrial ATP synthase) in neurons of the mouse model of mucopolysaccharidosis III B. *Mol Genet Metab* **90**: 393–401.
3. Ohmi, K, Greenberg, DS, Rajavel, KS, Ryazantsev, S, Li, HH and Neufeld, EF (2003). Activated microglia in cortex of mouse models of mucopolysaccharidoses I and IIIB. *Proc Natl Acad Sci USA* **100**: 1902–1907.
4. Ohmi, K, Kudo, LC, Ryazantsev, S, Zhao, HZ, Karsten, SL and Neufeld, EF (2009). Sanfilippo syndrome type B, a lysosomal storage disease, is also a tauopathy. *Proc Natl Acad Sci USA* **106**: 8332–8337.
5. McGlynn, R, Dobrenis, K and Walkley, SU (2004). Differential subcellular localization of cholesterol, gangliosides, and glycosaminoglycans in murine models of mucopolysaccharide storage disorders. *J Comp Neurol* **480**: 415–426.
6. Li, HH, Zhao, HZ, Neufeld, EF, Cai, Y and Gómez-Pinilla, F (2002). Attenuated plasticity in neurons and astrocytes in the mouse model of Sanfilippo syndrome type B. *J Neurosci Res* **69**: 30–38.
7. DiRosario, J, Divers, E, Wang, C, Etter, J, Charrier, A, Jukkola, P *et al.* (2009). Innate and adaptive immune activation in the brain of MPS IIIB mouse model. *J Neurosci Res* **87**: 978–990.
8. Villani, GR, Di Domenico, C, Musella, A, Cecere, F, Di Napoli, D and Di Natale, P (2009). Mucopolysaccharidosis IIIB: oxidative damage and cytotoxic cell involvement in the neuronal pathogenesis. *Brain Res* **1279**: 99–108.
9. Villani, GR, Gargiulo, N, Faraonio, R, Castaldo, S, Gonzalez Y Reyero, E and Di Natale, P (2007). Cytokines, neurotrophins, and oxidative stress in brain disease from mucopolysaccharidosis IIIB. *J Neurosci Res* **85**: 612–622.
10. Weber, B, Guo, XH, Kleijer, WJ, van de Kamp, JJ, Poorthuis, BJ and Hopwood, JJ (1999). Sanfilippo type B syndrome (mucopolysaccharidosis III B): allelic heterogeneity corresponds to the wide spectrum of clinical phenotypes. *Eur J Hum Genet* **7**: 34–44.
11. Yogalingam, G, Weber, B, Meehan, J, Rogers, J and Hopwood, JJ (2000). Mucopolysaccharidosis type IIIB: characterisation and expression of wild-type and mutant recombinant alpha-N-acetylglucosaminidase and relationship with sanfilippo phenotype in an attenuated patient. *Biochim Biophys Acta* **1502**: 415–425.
12. Rohrbach, M and Clarke, JT (2007). Treatment of lysosomal storage disorders: progress with enzyme replacement therapy. *Drugs* **67**: 2697–2716.
13. Muenzer, J and Fisher, A (2004). Advances in the treatment of mucopolysaccharidosis type I. *N Engl J Med* **350**: 1932–1934.
14. Pardridge, WM (2002). Drug and gene delivery to the brain: the vascular route. *Neuron* **36**: 555–558.
15. Berns, KI and Linden, RM (1995). The cryptic life style of adeno-associated virus. *Bioessays* **17**: 237–245.
16. Daya, S and Berns, KI (2008). Gene therapy using adeno-associated virus vectors. *Clin Microbiol Rev* **21**: 583–593.
17. Bankiewicz, KS, Forsayeth, J, Eberling, JL, Sanchez-Pernaute, R, Pivirotto, P, Bringas, J *et al.* (2006). Long-term clinical improvement in MPTP-lesioned primates after gene therapy with AAV-hAADC. *Mol Ther* **14**: 564–570.
18. Jacobson, SG, Boye, SL, Aleman, TS, Conlon, TJ, Zeiss, CJ, Roman, AJ *et al.* (2006). Safety in nonhuman primates of ocular AAV2-RPE65, a candidate treatment for blindness in Leber congenital amaurosis. *Hum Gene Ther* **17**: 845–858.
19. McPhee, SW, Janson, CG, Li, C, Samulski, RJ, Camp, AS, Francis, J *et al.* (2006). Immune responses to AAV in a phase I study for Canavan disease. *J Gene Med* **8**: 577–588.
20. Fu, H, Kang, L, Jennings, JS, Moy, SS, Perez, A, Dirosario, J *et al.* (2007). Significantly increased lifespan and improved behavioral performances by rAAV gene delivery in adult mucopolysaccharidosis IIIB mice. *Gene Ther* **14**: 1065–1077.
21. Fu, H, Muenzer, J, Samulski, RJ, Breese, G, Sifford, J, Zeng, X *et al.* (2003). Self-complementary adeno-associated virus serotype 2 vector: global distribution and broad dispersion of AAV-mediated transgene expression in mouse brain. *Mol Ther* **8**: 911–917.
22. Fu, H, Samulski, RJ, McCown, TJ, Picornell, YJ, Fletcher, D and Muenzer, J (2002). Neurological correction of lysosomal storage in a mucopolysaccharidosis IIIB mouse model by adeno-associated virus-mediated gene delivery. *Mol Ther* **5**: 42–49.

23. Fu, H, DiRosario, J, Kang, L, Muenzer, J and McCarty, DM (2010). Restoration of central nervous system alpha-N-acetylglucosaminidase activity and therapeutic benefits in mucopolysaccharidosis IIIB mice by a single intracisternal recombinant adeno-associated viral type 2 vector delivery. *J Gene Med* **12**: 624–633.
24. Desmaris, N, Verot, L, Puech, JP, Caillaud, C, Vanier, MT and Heard, JM (2004). Prevention of neuropathology in the mouse model of Hurler syndrome. *Ann Neurol* **56**: 68–76.
25. Heuer, GG, Passini, MA, Jiang, K, Parente, MK, Lee, VM, Trojanowski, JQ *et al.* (2002). Selective neurodegeneration in murine mucopolysaccharidosis VII is progressive and reversible. *Ann Neurol* **52**: 762–770.
26. Liu, G, Martins, I, Wemmie, JA, Chiorini, JA and Davidson, BL (2005). Functional correction of CNS phenotypes in a lysosomal storage disease model using adeno-associated virus type 4 vectors. *J Neurosci* **25**: 9321–9327.
27. McCarty, DM, DiRosario, J, Gulaid, K, Muenzer, J and Fu, H (2009). Mannitol-facilitated CNS entry of rAAV2 vector significantly delayed the neurological disease progression in MPS IIIB mice. *Gene Ther* **16**: 1340–1352.
28. Sands, MS and Haskins, ME (2008). CNS-directed gene therapy for lysosomal storage diseases. *Acta Paediatr Suppl* **97**: 22–27.
29. Fraldi, A, Hemsley, K, Crawley, A, Lombardi, A, Lau, A, Sutherland, L *et al.* (2007). Functional correction of CNS lesions in an MPS-IIIA mouse model by intracerebral AAV-mediated delivery of sulfamidase and SUMF1 genes. *Hum Mol Genet* **16**: 2693–2702.
30. Kaplitt, MG, Feigin, A, Tang, C, Fitzsimons, HL, Mattis, P, Lawlor, PA *et al.* (2007). Safety and tolerability of gene therapy with an adeno-associated virus (AAV) borne GAD gene for Parkinson's disease: an open label, phase I trial. *Lancet* **369**: 2097–2105.
31. Worgall, S, Sondhi, D, Hackett, NR, Kosofsky, B, Kekatpure, MV, Neyzi, N *et al.* (2008). Treatment of late infantile neuronal ceroid lipofuscinosis by CNS administration of a serotype 2 adeno-associated virus expressing CLN2 cDNA. *Hum Gene Ther* **19**: 463–474.
32. Lau, AA, Hopwood, JJ, Kremer, EJ and Hemsley, KM (2010). SGSH gene transfer in mucopolysaccharidosis type IIIA mice using canine adenovirus vectors. *Mol Genet Metab* **100**: 168–175.
33. Heldermon, CD, Ohlemiller, KK, Herzog, ED, Vogler, C, Qin, E, Wozniak, DF *et al.* (2010). Therapeutic efficacy of bone marrow transplant, intracranial AAV-mediated gene therapy, or both in the mouse model of MPS IIIB. *Mol Ther* **18**: 873–880.
34. Foust, KD, Nurre, E, Montgomery, CL, Hernandez, A, Chan, CM and Kaspar, BK (2009). Intravascular AAV9 preferentially targets neonatal neurons and adult astrocytes. *Nat Biotechnol* **27**: 59–65.
35. Duque, S, Joussemet, B, Riviere, C, Marais, T, Dubreil, L, Douar, AM *et al.* (2009). Intravenous administration of self-complementary AAV9 enables transgene delivery to adult motor neurons. *Mol Ther* **17**: 1187–1196.
36. Zincarelli, C, Soltys, S, Rengo, G and Rabinowitz, JE (2008). Analysis of AAV serotypes 1-9 mediated gene expression and tropism in mice after systemic injection. *Mol Ther* **16**: 1073–1080.
37. Gao, G, Vandenberghe, LH and Wilson, JM (2005). New recombinant serotypes of AAV vectors. *Curr Gene Ther* **5**: 285–297.
38. Akache, B, Grimm, D, Pandey, K, Yant, SR, Xu, H and Kay, MA (2006). The 37/67-kilodalton laminin receptor is a receptor for adeno-associated virus serotypes 8, 2, 3, and 9. *J Virol* **80**: 9831–9836.
39. Halbert, CL, Miller, AD, McNamara, S, Emerson, J, Gibson, RL, Ramsey, B *et al.* (2006). Prevalence of neutralizing antibodies against adeno-associated virus (AAV) types 2, 5, and 6 in cystic fibrosis and normal populations: Implications for gene therapy using AAV vectors. *Hum Gene Ther* **17**: 440–447.
40. Chirmule, N, Propert, K, Magosin, S, Qian, Y, Qian, R and Wilson, J (1999). Immune responses to adenovirus and adeno-associated virus in humans. *Gene Ther* **6**: 1574–1583.
41. Calcedo, R, Vandenberghe, LH, Gao, G, Lin, J and Wilson, JM (2009). Worldwide epidemiology of neutralizing antibodies to adeno-associated viruses. *J Infect Dis* **199**: 381–390.
42. Braulke, T and Bonifacino, JS (2009). Sorting of lysosomal proteins. *Biochim Biophys Acta* **1793**: 605–614.
43. Bevan, AK, Hutchinson, KR, Foust, KD, Braun, L, McGovern, VL, Schmelzer, L *et al.* (2010). Early heart failure in the SMNΔ7 model of spinal muscular atrophy and correction by postnatal scAAV9-SMN delivery. *Hum Mol Genet* **19**: 3895–3905.
44. Zolotukhin, S, Byrne, BJ, Mason, E, Zolotukhin, I, Potter, M, Chesnut, K *et al.* (1999). Recombinant adeno-associated virus purification using novel methods improves infectious titer and yield. *Gene Ther* **6**: 973–985.
45. Li, HH, Yu, WH, Rozengurt, N, Zhao, HZ, Lyons, KM, Anagnostaras, S *et al.* (1999). Mouse model of Sanfilippo syndrome type B produced by targeted disruption of the gene encoding alpha-N-acetylglucosaminidase. *Proc Natl Acad Sci USA* **96**: 14505–14510.
46. Lijam, C, Paylor, R, McDonald, MP, Crawley, JN, Deng, CX, Herrup, K *et al.* (1997). Social interaction and sensorimotor gating abnormalities in mice lacking Dvl1. *CelCl* **90**: 895–905.
47. Thompson, JN and Nowakowski, RW (1991). Enzymatic diagnosis of selected mucopolysaccharidoses: Hunter, Morquio type A, and Sanfilippo types A, B, C, and D, and procedures for measurement of 35SO4-glycosaminoglycans. In: Hommes FA (ed). *Techniques in Diagnostic Human Biochemical Genetics-A Laboratory Manual.* Wiley-Liss: New York. pp 567–586.
48. van de Lest, CH, Versteeg, EM, Veerkamp, JH and van Kuppevelt, TH (1994). Quantification and characterization of glycosaminoglycans at the nanogram level by a combined azure A-silver staining in agarose gels. Anal Biochem **221**: 356–361.
49. de Jong, JG, Wevers, RA, Laarakkers, C and Poorthuis, BJ (1989). Dimethylmethylene blue-based spectrophotometry of glycosaminoglycans in untreated urine: a rapid screening procedure for mucopolysaccharidoses. *Clin Chem* **35**: 1472–1477.